JOURNAL OF BACTERIOLOGY, Jan. 2011, p. 367–376 Vol. 193, No. 2
0021-9193/11/$12.00 doi:10.1128/JB.01095-10


# Differences in MinC/MinD Sensitivity between Polar and Internal Z Rings in *Escherichia coli*[▽]

Bang Shen and Joe Lutkenhaus*

*Department of Microbiology, Molecular Genetics and Immunology, University of Kansas Medical Center, Kansas City, Kansas 66160*

Received 14 September 2010/Accepted 9 November 2010

**In *Escherichia coli* the Z ring has the potential to assemble anywhere along the cell length but is restricted to midcell by the action of negative regulatory systems, including Min. In the current model for the Min system, the MinC/MinD division inhibitory complex is evenly distributed on the membrane and can disrupt Z rings anywhere in the cell; however, MinE spatially regulates MinC/MinD by restricting it to the cell poles, thus allowing Z ring formation at midcell. This model assumes that Z rings formed at different cellular locations have equal sensitivity to MinC/MinD in the absence of MinE. However, here we report evidence that differences in MinC/MinD sensitivity between polar and nonpolar Z rings exists even when there is no MinE. MinC/MinD at proper levels is able to block minicell production in Δ*min* strains without increasing the cell length, indicating that polar Z rings are preferentially blocked. In the FtsZ-I374V strain (which is resistant to $MinC^C$/MinD), wild-type morphology can be easily achieved with MinC/MinD in the absence of MinE. We also show that MinC/MinD at proper levels can rescue the lethal phenotype of a *min slmA* double deletion mutant, which we think is due to the elimination of polar Z rings (or FtsZ structures), which frees up FtsZ molecules for assembly of Z rings at internal sites to rescue division and growth. Taken together, these data indicate that polar Z rings are more susceptible to MinC/MinD than internal Z rings, even when MinE is absent.**

Rod-shaped bacteria, such as *Escherichia coli*, divide precisely at midcell through the action of the divisome to produce two daughter cells. Formation of the divisome is initiated with Z ring assembly, which consists of FtsZ polymers attached to the inner membrane through interaction with membrane-associated division proteins, such as FtsA and ZipA (5, 13, 31). Z ring formation is a critical step in cytokinesis and is subject to tight spatial and temporal controls to ensure it occurs at the right time and place (1, 27). In *E. coli*, two negative regulatory systems, Min and NO (for *n*ucleoid *o*cclusion), are involved in positioning the Z ring to midcell. The Min system blocks Z ring assembly at cell poles, which prevents polar divisions and the generation of chromosome-free minicells and nucleoid-containing cells that are heterogeneous in length (7, 9, 27). The NO system prevents Z ring formation over the nucleoid, although inactivation of the known NO factor (SlmA) does not have any obvious phenotype during balanced growth (3, 41). Although neither system is essential for cell growth, knocking out both systems is lethal, because cell division fails to occur due to the inability to assemble a mature Z ring (3).

The Min system is found in a variety of bacteria and has been extensively studied in the Gram-negative bacterium *E. coli* and the Gram-positive bacterium *Bacillus subtilis*. In *E. coli*, the Min system consists of three proteins: MinC, MinD, and MinE (9). MinC is a division inhibitor that antagonizes Z ring assembly (19). MinD is a membrane-associated ATPase that recruits MinC to the membrane and activates MinC (15, 20). Together, MinC and MinD form a potent division inhibitory complex on the membrane that is able to prevent Z ring formation. MinE confers topological specificity to this system by restricting MinC/MinD to the cell poles, which allows a Z ring to form at midcell. MinE does so by imposing a periodic pole-to-pole oscillation on MinC/MinD through stimulation of the ATPase activity of MinD, which releases MinC/MinD from the membrane (11, 14, 15, 17, 18, 32, 33). The detailed molecular mechanism for the Min oscillation is still under investigation (22, 26), but the net result of such a dynamic pattern is that the time-averaged concentration of the MinC/MinD inhibitor is highest at cell poles and lowest at midcell (28).

As the effector of the Min system, MinC has two functional domains (the N-terminal domain, $MinC^N$, and the C-terminal domain, $MinC^C$), both of which interact with FtsZ to antagonize Z ring assembly (16, 37). $MinC^N$ interacts with the H-10 helix of FtsZ at the dimer interface to break FtsZ polymers (36); $MinC^C$, along with MinD, binds to the extreme C-terminal tail of FtsZ to displace FtsA and/or ZipA from the Z ring (35). The two domains work synergistically and both domains of MinC are essential for the proper function of the Min system, because mutations inactivating either domain of MinC (MinC-G10D and MinC-R172A) disrupt Min function, as evidenced by minicell production (44).

Recently, we isolated mutations in FtsZ that specifically disrupt the interaction between FtsZ and each of the domains of MinC (35, 36). Although these FtsZ mutants behave very similarly to the MinC mutants (MinC-G10D and MinC-R172A, which inactivate $MinC^N$ and $MinC^C$, respectively) in affecting the responsiveness of FtsZ to MinC in many aspects, there is one difference. As mentioned above, MinC-G10D or MinC-R172A reduces Min function significantly, as these mutations fail to complement the Δ*min* strain. However, in the two FtsZ mutant strains that were studied in detail, BSZ374

* Corresponding author. Mailing address: Department of Microbiology, Molecular Genetics and Immunology, University of Kansas Medical Center, Kansas City, KS 66160. Phone: (913) 588-7054. Fax: (913) 588-7295. E-mail: jlutkenh@kumc.edu.

▽ Published ahead of print on 19 November 2010.

(FtsZ-I374V, which disrupts the $MinC^C$/MinD-FtsZ interaction) and BSZ280D (FtsZ-N280D, which decreases the $MinC^N$-FtsZ interaction), the Min system appears to function properly, since minicells were not produced. This is surprising, because as we have shown before that both FtsZ mutants have significant MinC/MinD resistance (36) and would be expected to produce minicells. Why do MinC mutants make minicells but the FtsZ mutants do not, even though they affect the MinC-FtsZ interaction similarly? This is puzzling, and no suitable explanation is apparent. This is particularly true for the BSZ374 strain, whereas for the BSZ280D strain, as we have discussed previously (36), the reduced activity of the mutant FtsZ protein may partially counteract its MinC/MinD resistance and therefore limit minicell production. However, it is very hard to believe that this is the only reason for the nonminicelling phenotype, because the vast majority of the BSZ280D cells appear to be wild type.

In investigating the nonminicelling phenotype of the two FtsZ mutant strains, we found that Z rings that form at different cellular locations display different sensitivities to MinC/MinD, even in the absence of MinE. This observation is contradictory to the current view of the Min system, for which it is generally assumed that all Z rings are equivalent and have the same sensitivity to MinC/MinD in the absence of MinE. Here, we provide evidence showing that polar and internal Z rings (midcell ones and nonpolar ones between nucleoids in long cells) display different sensitivities to MinC/MinD in a variety of strain backgrounds, and we discuss how this may be linked to the nonminicelling phenotype of the two FtsZ mutants.

## MATERIALS AND METHODS

**Strains and plasmids.** The Δ*min* Δ*slmA* double mutant strains were made by P1 phage-mediated transduction. P1 phage grown on W3110 *slmA*::*cat* was used to transduce *slmA*::*cat* into the *min*::*kan* strains S4, BSM374, BSM280, and BSM23 to give the double mutants S14, S16, S19, and S20, respectively. All other strains were described previously (36). The Δ*min* Δ*slmA* double mutants were constructed and maintained at 42°C in LB medium; all other strains were grown at 37°C on LB plates or in LB medium unless otherwise indicated. The plasmid pBANG84 was constructed by replacing the *tac* promoter on the plasmid pBANG59 (35) with the *trc* promoter from pDSW210. The P*trc*+*lacI*$^q$ region from pDSW210 (40) was PCR amplified (using the primers 5′-lacIq-BglII, GCAGATCTACGATGTCGCAGAG TATGCC, and 3′-LacIq-MCS, GAATTGGGACAACTCCAGTG) and cloned into pBANG59 digested with BglII and EcoRI. The plasmid pBS31 was constructed by cloning the *sulA* fragment obtained by SstI and HindIII digestion of pA3 (8) into pDSW208 (40). To make the plasmid pBANG55, which expresses the fusion (MinC-MTS) of MinC and membrane-targeting sequence (MTS) of *B. subtilis* MinD ($_{Bs}MinD_{248–268}$), a PCR product containing *minC-MTS* obtained by amplification of *E. coli minC* with primers 5′-MinC-SstI (GGAGCTCGCTAATTGAGTAAGGCC AGGATG) and 3′-MinC-BsMTS-HindIII (CGAAGCTTTTAAGATCTTACTCC GAAAAATGACTTAATCTTAGCCATCATTCCTTTGTTTTGCTCTTCAAGC ACCCCGCCTCCATTTAACGGTTGAACGGTC) was digested with SstI and HindIII and cloned into similarly digested pDSW208. pBANG77 was the same as pBANG55 except that the residues $F_{263}F_{264}$ in the MTS were mutated to $D_{263}D_{264}$ to disrupt the membrane targeting.

**Cell morphology analysis.** Overnight cultures were diluted 1,000-fold in LB medium (supplemented with proper antibiotics) and grown at 37°C to an optical density at 600 nm ($OD_{600}$) of ≈0.4. These exponentially growing cultures were diluted 100-fold again into fresh LB medium with the indicated concentrations of isopropyl-β-D-thiogalactopyranoside (IPTG) and grown for another 2 to 3 h to reach an $OD_{600}$ of 0.4. The cells were then fixed with 0.2% glutaraldehyde for subsequent determination of polar divisions and cell length analysis based on phase-contrast microscopy.

**Immunofluorescence microscopy examining the cellular localization of FtsZ.** To check FtsZ localization in strain BSM374/pBANG59 cultured with or without 1 mM IPTG, an overnight culture was diluted 1,000-fold into LB medium containing spectinomycin (Spc) and cells were grown to an $OD_{600}$ of ≈0.4 at 37°C. This culture was diluted 100-fold again into LB-Spc medium with or without 1 mM IPTG and grown to an $OD_{600}$ of 0.4. The cells were then fixed and immunostained using FtsZ antiserum as previously described (35). To examine the effect of MinC/MinD on FtsZ localization in the Δ*min* Δ*slmA* double mutant strain S16 grown at low temperature, a colony of S16/pBANAG59 cells grown at 42°C was streaked on an LB plate (supplemented with kanamycin [Kan], chloramphenicol [Cam], and Spc) containing 50 μM IPTG and then incubated at 30°C for 6 h. Cells were then scraped off the plate and fixed for subsequent immunostaining. As a control, the same colony was also streaked onto a plate without IPTG and incubated at 42°C for 3 h, and then shifted to 30°C and grown for another 2.5 h. Cells were then collected and stained in the same way as above. In the latter case, cells from plates instead of from liquid culture were used, because S16/pBANAG59 cells cultured in LB medium (at 30°C) had a mild filamentation phenotype even under the optimal IPTG induction conditions. The same cells grown on plates with 50 μM IPTG are shorter without significant filamentation.

## RESULTS

**Bypass of MinE for spatial regulation of cytokinesis by MinC/MinD in the FtsZ-I374V strain.** Microscopic examination of BSM374/pBANG59 (*ftsZ-I374V min*::*kan*/P*lac*::*minCD*) cells growing under different IPTG concentrations revealed an IPTG-dependent change in cellular morphology. With no or very low levels of IPTG (≤10 μM) this strain, as expected, displayed a typical Δ*min* morphology, with minicells and nucleoid-containing cells that were heterogeneous in length (Fig. 1A, B, and E). At IPTG concentrations in the ~50 to 100 μM range, this strain still displayed the characteristic heterogeneous cell length distribution of a typical Δ*min* strain, but minicell production was dramatically decreased (Fig. 1A and B). At this IPTG concentration the average cell length and the cell length distribution were similar to the same strain without IPTG (Fig. 1A and data not shown). Thus, the level of MinC/MinD produced by this concentration of IPTG almost completely blocked polar divisions as evidenced by the decreased minicell production, even though nonpolar (internal) divisions must not have been affected. A further increase in the IPTG concentration to 1 mM to induce a higher level of MinC/MinD produced a wild-type morphology (compare Fig. 1C and D); there were no minicells, and the average cell length (3.9 μm for BSM374/pBANG59 grown with 1 mM IPTG and 3.7 μm for cells of the $Min^+$ strain BSZ374) and cell length distribution were very close to that of $Min^+$ cells (Fig. 1A to E). In this population, cell division occurs at midcell, and immunostaining revealed that these cells did not have detectable polar Z rings. Most Z rings were at midcell, although occasionally an off-center ring was observed in rare long cells (Fig. 1H). These results were very surprising, because these cells lack MinE for directing MinC/MinD to the cell poles. The evidence, however, clearly indicates that MinC/MinD eliminates polar Z rings without inhibiting midcell ones. Thus, in the FtsZ-I374V strain, the appropriate level of MinC/MinD was as effective as the fully intact Min system in spatially regulating Z ring formation. This change in morphology was truly dependent upon MinC/MinD, since it did not occur if the plasmid contained the *minC* mutation G10D (Fig. 1A), which reduces the inhibitory activity of the N-terminal domain of MinC (16, 19).

To further investigate this phenomenon we used another plasmid, pBANG78 (35), which can produce higher levels of MinC/MinD than pBANG59. Induction of BSM374/pBANG78 with IPTG produces even more extensive changes in cell morphology than observed with BSM374/pBANG59. In

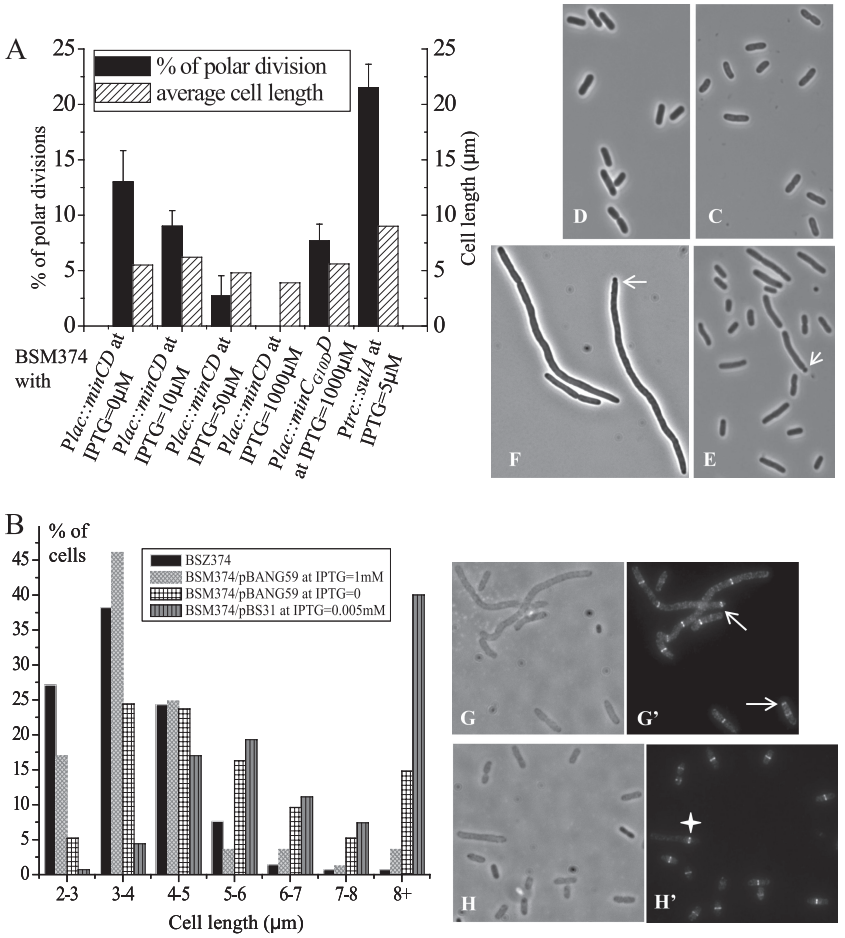


FIG. 1. The effects of MinC/MinD induction on minicell production and cell length distribution of the BSM374 strain. (A) Percentages of polar divisions and average cell length of the BSM374 strain (*ftsZ-I374V min*::*kan*) under the indicated conditions: BSM374/pBANG59 (P*lac*::*minCD*) with IPTG at 0 μM; BSM374/pBANG59 with IPTG at 10 μM; BSM374/pBANG59 with IPTG at 50 μM; BSM374/pBANG59 with IPTG at 1,000 μM; BSM374/pBANG59-G10D with IPTG at 1,000 μM; BSM374/pBS31 (P*trc*::*sulA*) with IPTG at 5 μM. The percentage indicates the number of visible polar divisions compared to the the number of total divisions for each strain. (B) Cell length distributions of the strains in panel A. (C to F) Phase-contrast microscopic images of select strains to demonstrate the morphology. (C) BSZ374 (*min*$^+$); (D) BSM374/pBANG59 in the presence of 1 mM IPTG; (E) BSM374/pBANG59 without IPTG; (F) BSM374/pBS31with 5 μM IPTG. (G and H) Immunostaining to examine FtsZ localization in BSM374/pBANG59 cells with IPTG at 0 μM (G and G′) and BSM374/pBANG59 cells with IPTG at 1 mM (H and H′). Images in panels G and H are phase-contrast images of the corresponding fluorescent images shown in panels G′ and H′. Arrows in panels E to G′ indicate polar divisions (E and F) or polar Z rings (G′), and the star in panel H′ indicates an off-center but nonpolar Z ring.

the absence of IPTG, BSM374/pBANG78 cells behaved like a typical Δ*min* strain, even though fewer minicells were produced (data not shown), probably because of a higher basal level of MinC/MinD from this plasmid (this basal level is sufficient to prevent introduction of this plasmid into an FtsZ– wild-type (WT) Δ*min* strain, such as S4 [35]). In the presence of 5 to 10 μM IPTG, the cell morphology approached that of a WT strain; cells divided in the middle and the cell length distribution was more homogeneous, with the majority of cells falling within the WT cell length distribution range. When MinC/MinD was induced to an even higher level with IPTG concentrations above 20 μM, cells became filamentous and died (data not shown) (35). Together, these data clearly demonstrate that in the BSM374 strain polar Z rings are more susceptible to MinC/MinD than are internal (nonpolar) Z rings, and the requirement of MinE for the spatial regulation of MinC/MinD can be completely bypassed. The observed filamentation also emphasizes that although FtsZI374V is resistant to MinC$^C$/MinD, it is still susceptible to MinC$^N$ when it is produced at high levels.

To see whether blocking minicell production without causing the filamentation observed with MinC/MinD is a general property shared by all division inhibitors, another division inhibitor (SulA) was expressed in the BSM374 strain, and the change in cell morphology was monitored at various levels of induction. SulA is a cytoplasmic protein induced as part of the SOS response and is a well-characterized inhibitor of cell division that acts by sequestering FtsZ (4, 8, 21). In contrast to the Min system, in which the division-inhibitory activity is topologically regulated, SulA does not display topological specificity in blocking division. As shown in Fig. 1A and F, induction of SulA at a level that causes partial inhibition of division and mild filamentation did not block polar divisions. This indicates that unlike MinC/MinD, SulA does not preferentially

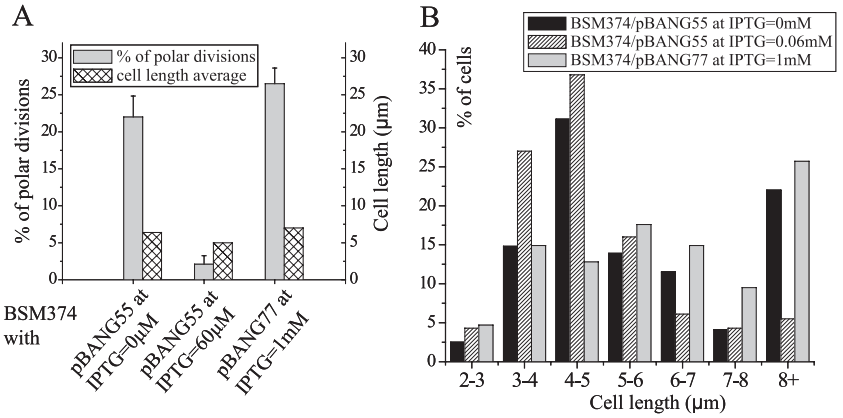


FIG. 2. The effects of MinC-MTS and MinC induction on minicell production and cell length distribution in the BSM374 strain. (A) Minicell production and average cell length of BSM374 (*ftsZ-I374V min*::*kan*) cells following MinC or MinC-MTS induction. Strains and conditions: BSM374/pBANG55 (P*trc*::*minC-MTS*) with IPTG at 0 μM; BSM374/pBANG55 (P*trc*::*minC-MTS*) with IPTG at 60 μM; BSM374/pBANG77 (P*trc*::*minC-MTS* with an $F_{263}F_{264}$-to-DD mutation in the MTS to disrupt membrane localization) with IPTG at 1 mM. (B) Cell length distributions of the three strains shown in panel A.

inhibit polar divisions and therefore does not distinguish between Z rings present at different cellular locations.

**Membrane association but not MinD is required for MinC to differentially affect polar and internal divisions.** The above tests showed that MinC/MinD, but not SulA, can block minicell formation in the Δ*min* strain BSM374 without causing filamentation. One difference between these two division inhibitors is that MinC/MinD is at the membrane, where Z rings are attached, whereas SulA is in the cytoplasm. To explore the requirements for MinC to differentially affect polar and internal Z rings, we constructed a membrane-associated version of MinC (MinC-MTS) by fusing it to the membrane-targeting sequence of *B. subtilis* MinD, $_{Bs}MinD_{248–268}$(pBANG55) (38). For a control we introduced two point mutations in the MTS ($F_{263}F_{264}$ to $D_{263}D_{264}$), which completely prevented the membrane association of MinC-MTS as revealed by green fluorescent protein (GFP) tagging to the N terminus of MinC-MTS (data not shown), to yield pBANG77. These two plasmids were introduced into the BSM374 strain, and the cell morphology was examined following induction with IPTG.

As shown in Fig. 2, induction of MinC-MTS with about 60 to 100 μM IPTG reduced minicell production in the BSM374 strain significantly without increasing the cell length. Actually, the average cell length decreased and the cell length distribution became more homogeneous, even though a completely wild-type morphology was not achieved. When MinC-MTS was induced to a higher level, it blocked all divisions and caused filamentation (data not shown). In contrast to the effects of MinC-MTS, the membrane binding mutant of MinC-MTS never blocks minicell production without causing filamentation. The effect is very similar to SulA in that minicells are still produced at the level that causes mild filamentation (Fig. 2). These results indicate that MinD is not absolutely required for MinC to distinguish internal Z rings from polar Z rings but that MinC has to be on the membrane to achieve this effect. On the other hand, a wild-type morphology can be readily achieved with MinC/MinD but not with MinC-MTS, suggesting that MinD plays other roles in addition to recruiting MinC to the membrane.

**Differential MinC/MinD sensitivity between polar and internal Z rings in other strains.** When we first observed the above morphology changes with the BSM374 strain upon MinC/MinD or MinC-MTS induction, we assumed that it was a unique property of the FtsZ-I374V mutant. To check this, similar tests were done in other strains with different genetic backgrounds. First, we tested two FtsZ-WT strains, S4 (W3110; *leu*::Tn*10*, *min*::*kan*) and S22 (MG1655; *min*::*kan*). Both strains contained the plasmid pBANG59 (P*lac*::*minCD*) and displayed similar morphological changes upon MinC/MinD induction. Induction with low or no IPTG (≤10 μM) caused a typical $Min^-$ phenotype (the results for the S4 strain are shown in Fig. 3). As the MinC/MinD level was increased, minicell production was gradually reduced without the cells getting any longer. In contrast to the BSM374 strain results, however, this elimination of minicell production without an increase in cell length only occurred over a very narrow range of MinC/MinD induction (for example, IPTG at 20 to 25 μM for S4/pBANG59). In this narrow range, minicell formation was almost completely blocked, but the average cell length and cell length distribution were similar to a typical Δ*min* strain (Fig. 3A and B). If the induction of MinC/MinD is above this window, filamentation starts to occur.

These results indicate that MinC/MinD can stop minicell formation in these two FtsZ-WT strains without causing filamentation. However, the range of MinC/MinD induction that produces this is very narrow. In addition, no MinC/MinD induction conditions were found that produced a WT morphology in these Δ*min* cells. These differences between the results with FtsZ-WT strains and the BSM374 strain are probably due to the fact that FtsZ-WT is more sensitive to MinC/MinD than FtsZ-I374V. The broader MinC/MinD induction range that blocks minicell formation without inducing filamentation in the FtsZ-I374V mutant suggests that the difference in MinC/MinD sensitivity between polar and internal Z rings is much greater in this mutant than in FtsZ-WT strains (discussed below).

We also examined two other FtsZ mutant strains, BSM280D (*ftsZ-N280D min*::*kan*) and BSM23 (*ftsZ-23 min*::*kan*), for

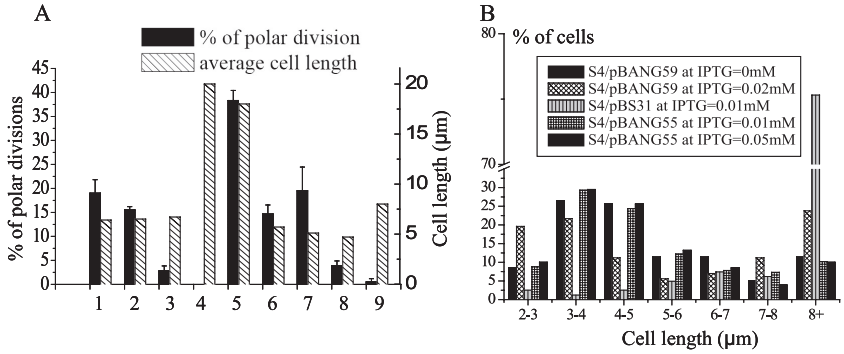


FIG. 3. MinC/MinD and MinC-MTS block minicell production in the *ftsZ-WT* strain. (A) Percentages of polar divisions and average cell lengths of the S4 (*min*::*kan*) strain containing plasmids expressing MinC/MinD, SulA, or MinC-MTS at different induction levels. The strains and growth conditions were as follows: 1 to 4, S4/pBANG59 (P*lac*::*minCD*) with IPTG at 0, 10, 20, and 50 μM, respectively; 5, S4/pBS31 (P*trc*::*sulA*) with IPTG at 10 μM; 6, S4/pBANG59-G10D with IPTG at 1,000 μM; 7 to 9, S4/pBANG55 (P*trc*::*minC-MTS*) with IPTG at 10, 50, and 100 μM, respectively. (B) Cell length distributions of the indicated strains.

their response to MinC/MinD. BSM280D/pBANG59 responds to MinC/MinD induction similarly to S4/pBANG59 (data not shown), but the minimal IPTG concentration required to stop minicell formation in this strain was higher (about 100 μM). In addition, there was only a small concentration range for MinC/MinD induction (IPTG, ≈100 to 200 μM) that blocked minicell formation without causing significant filamentation in the BSM280 strain. However, such tests in this strain are more difficult to interpret. A key point of these tests is the existence of a MinC/MinD induction level that stops minicell production without causing any filamentation. Unfortunately, the BSM280D strain without any plasmid displays a mild filamentation phenotype and broader cell length distribution compared to a typical Δ*min* strain, such as S4 (36). Nevertheless, our results indicate that the different MinC/MinD sensitivities between polar and internal Z rings also exist in the BSM280D strain.

In contrast to the strains tested so far, BSM23/pBANG59 was not affected by MinC/MinD induction. Minicells were produced at all IPTG concentrations, and there was no significant change in morphology at different levels of MinC/MinD induction (data not shown). This is consistent with this strain being insensitive to MinC/MinD due to the presence of the *ftsZ23* allele, which is resistant to both domains of MinC (36). The results also support our conclusion that the prevention of minicell production observed in the other strains is indeed due to the action of MinC/MinD.

We also tested MinC-MTS, the membrane binding mutant form of MinC-MTS, and SulA in the S4 strain. As shown in Fig. 3, similar to MinC/MinD, expression of MinC-MTS in this strain at the appropriate level (IPTG concentrations of 50 to 100 μM) was also able to block minicell production without significantly changing the cell length. Whereas for SulA and the membrane binding mutant version of MinC-MTS, just as in the BSM374 strain, neither of these constructs was able to differentially affect polar and internal Z rings, because polar divisions were still robust at induction levels that caused mild filamentation (Fig. 3 and data not shown). These results again suggest that MinD is not absolutely required for MinC to differentially affect polar and internal Z rings but that MinC must be on the membrane.

Taken together, these data indicate that the different MinC/MinD (and MinC-MTS) sensitivities between polar and internal Z rings are not unique to the FtsZ-I374V mutant but exist in a variety of strain backgrounds as long as the strain is not completely resistant (such as FtsZ-23) to MinC/MinD.

**MinC/MinD is able to rescue the growth defect of *min slmA* double mutants.** As mentioned earlier, neither *min* nor s*lmA* is essential. However, inactivation of both is lethal at low temperatures (≤30°C), because the cells fail to assemble functional Z rings and therefore cannot divide. The synthetic lethal phenotype of the *min slmA* double mutant can be rescued under several conditions: increased FtsZ, growth in minimal medium, and growth at high temperature (3; S. Du and J. Lutkenhaus, unpublished data). If the double mutant is grown in minimal medium, such as M9, or in rich medium at a high temperature, such as 42°C, the cells are able to divide and form regular-sized colonies. In rich medium at low temperatures, such as 30°C, a 1- to 2-fold increase in FtsZ can also rescue the growth of the cells. In all cases a minicelling phenotype is observed under suppression conditions. It seems, therefore, that the problem of the Δ*min* Δ*slmA* double mutant at low temperature is that FtsZ molecules in the cell are distributed among many FtsZ structures (3) but none of them are able to mature into a functional Z ring. Therefore, increasing the FtsZ level in the cell allows complete Z rings to form and can rescue the growth of this double mutant. In addition, it is likely that growing the double mutant at high temperature or in minimal medium also increases the FtsZ protein level or activity and therefore restores growth (in support of this, the viability of the ΔRodZ mutant, which normally requires extra FtsZ to grow in rich medium at low temperatures, is also improved by growth on minimal medium or at 42°C on LB plates [2]).

We wanted to test whether MinC/MinD at some level can rescue the growth of the Δ*min* Δ*slmA* mutant. The hypothesis was that if MinC/MinD can distinguish polar Z rings from internal Z rings and selectively disrupt the polar ones, it may free up sufficient FtsZ molecules so that enough FtsZ is available to assemble complete Z rings at internal sites. If so, MinC/MinD should rescue the growth of the double mutant. To test this possibility, we introduced the plasmid expressing MinC/MinD (pBANG84/P*trc*::*minCD*) into four different *min*

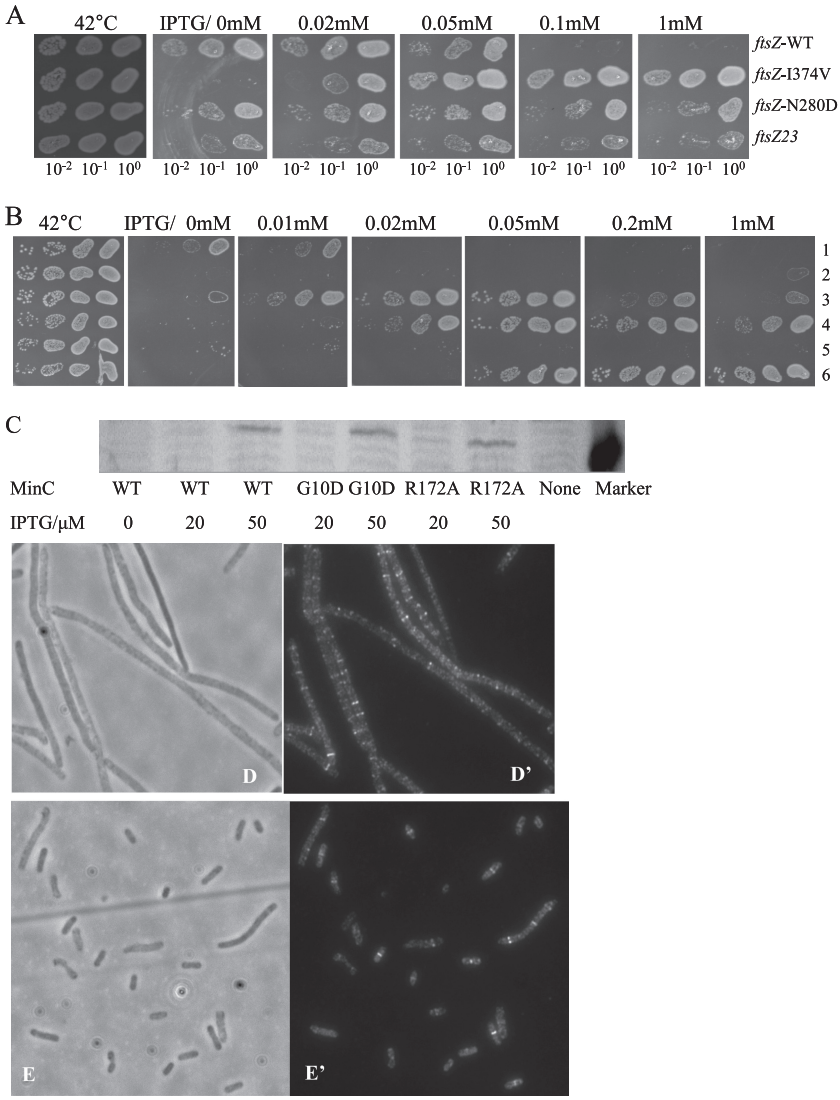


FIG. 4. Rescue of the Δ*min* Δ*slmA* double mutant by MinC/MinD at low temperature. (A) Rescue of the double mutant containing the indicated *ftsZ* alleles by MinC/MinD. Strains harboring the plasmid pBANG84 (P*trc*::*minCD*) were serially diluted 10-fold and spotted on LB plates supplemented with Spc, Kan, Cam, and the indicated concentration of IPTG at 30°C. A control panel contained cells grown at 42°C with the antibiotics but without IPTG. (B) The abilities of MinC/MinD and its derivatives to rescue the Δ*min* Δ*slmA* double mutant containing *ftsZ-WT* or *ftsZ-I374V*. The test was performed as for that in panel A, and the strains were as follows: first row, S14 (*ftsZ-WT min*::*kan slmA*::*cat*)/pBANG59 (P*lac*::*minCD*); second row, S14/pBANG59-G10D (P*lac*::*minC*$_{G10D}$*D*); third row, S14/pBANG59-R172A (P*lac*::*minC*$_{R172A}$*D*); fourth row, S16 (*ftsZ-I374V min*::*kan slmA*::*cat*)/pBANG59; fifth row, S16/pBANG59-G10D; sixth row, S16/pBANG59-R172A. (C) Western blot showing the levels of MinC and its derivatives from the plasmid pBANG59 in strain S16. Cells with the indicated constructs were grown with the indicated concentrations of IPTG at 42°C to an $OD_{600}$ of ≈0.1, and the cultures were then shifted to 30°C and grown to and $OD_{600}$ of 0.4 for subsequent immunoblot analysis. The S16 strain grown at 42°C without the plasmid was used as a Min$^-$ control. (D and E) Immunofluorescence microscopy to examine the localization of FtsZ in strain S16/pBANG59 grown with (E) or without (D) IPTG at 30°C. A colony grown at 42°C was streaked on a plate containing 50 μM IPTG (E) and incubated at 30°C for 6 h. Cells were then scraped off the plate and fixed for subsequent immunostaining. As a control, the same colony was also streaked onto a plate without IPTG (D) and incubated at 42°C for 3 h, then shifted to 30°C and grown for another 2.5 h. Cells were then collected and stained in the same way as described above. Panels D′ and E′ are the fluorescent images showing the localization of FtsZ in cells with the above treatments; panels D and E are the corresponding phase-contrast images.

*slmA* mutants and examined their growth at different levels of MinC/MinD induction. As shown in Fig. 4A, low induction levels of MinC/MinD rescued the growth of S14 (W3110; *min*::*kan slmA*::*cat*) at 30°C, but high inductions levels did not. In the case of S16 (BSZ374; *min*::*kan slmA*::*cat*), high levels (IPTG at ≥50 μM) of MinC/MinD rescued growth but low levels did not, consistent with the fact that FtsZ-I374V is more resistant to MinC/MinD than FtsZ-WT. For S19 (BSZ280D; *min*::*kan slmA*::*cat*), it seems like a broad range of MinC/MinD levels improve growth somewhat, but complete rescue is never achieved. As for S20 (BSZ23; *min*::*kan slmA*::*cat*), no condition was found to efficiently rescue colony formation; even though MinC/MinD induction helped growth somewhat, it was never to the point at which isolated colonies were formed.

To investigate this rescue assay further, we used two MinC mutants (G10D and R172A) to check their abilities to rescue the double mutants S14 and S16. To this end, the plasmid pBANG59 (P*lac*::*minCD*) was used, since it can induce MinC/MinD to a slightly higher level than the plasmid pBANG84. Consistent with the higher level of MinC/MinD from this plasmid, the basal expression of MinC/MinD was above the upper limit to rescue the S14 strain (Fig. 4B, first row). However, the S16 strain was efficiently rescued by this plasmid at IPTG concentrations above 20 μM (Fig. 4B, fourth row). When the MinC-G10D mutation was present on plasmid pBANG59, it no longer rescued the double mutants under all conditions tested (Fig. 4B, second and fifth rows), and its inability to rescue was not due to reduced expression or stability of this mutant, as revealed by Western blot analysis (Fig. 4C). This suggests that $MinC^N$ plays a critical role in rescuing these mutants and is consistent with the above observation that the S19 strain (*ftsZ-N280D min*::*kan slmA*::*cat*) cannot be efficiently rescued by MinC/MinD, since the activity of $MinC^N$ is dramatically reduced in this strain. pBANG59 harboring the MinC-R172A mutation was able to rescue both strains (S14 and S16) (Fig. 4B, third and sixth rows), further confirming that $MinC^N$ plays a more important role than $MinC^C$. Interestingly, these strains were only rescued within a limited range of $MinC^{R172A}$/MinD induction levels. For example, S14 was rescued at IPTG concentrations between 10 and 50 μM (Fig. 4, third row). Below this level S14 was not rescued, and it was killed by $MinC^{R172A}$/MinD above this range.

Microscopic examination revealed that when growth of the double mutant was efficiently rescued by MinC/MinD, the cells were close to (if not less heterogeneous than) typical Δ*min* cells in cell length distribution (Fig. 4E), but they did not make minicells. This is consistent with the hypothesis that MinC/MinD eliminates polar Z rings/FtsZ structures to increase the FtsZ supply for making internal Z rings. This result is also consistent with the notion that extra FtsZ is the key for rescuing the growth of these cells, although in this case, the increase in FtsZ is due to local redistribution rather than an overall increase in the level of FtsZ. Interestingly, rescue of the double mutant by an actual increase in the level of FtsZ correlates with minicell production (about 10 to 15% of the total divisions are polar when the S16 strain is rescued by FtsZ-I374V with the plasmid pBANG112 at 30°C), which is very different than rescue by MinC/MinD. These findings add further support to the idea that the rescue by MinC/MinD is due to the elimination of polar Z rings/FtsZ structures.

Lastly, we used immunostaining to examine FtsZ localization in the double mutant under conditions in which it was or was not rescued by MinC/MinD. One example is shown in Fig. 4. When the cells were grown under conditions at which they were not rescued (S16/pBANG59 with IPTG at 0 μM), they failed to divide and formed very long filaments (Fig. 4D). FtsZ staining showed that many Z rings and FtsZ structures with different staining densities were present throughout the filaments (Fig. 4D′), but apparently none of these matured into functional Z rings that could support division. In contrast, when the cells were grown under conditions that rescued growth (S16/pBANG59 with IPTG at 50 μM), they became shorter and had the typical morphology of a Δ*min* mutant (Fig. 4E) but without minicell production. Immunostaining indicated that most cells have only one or two Z rings at internal positions (Fig. 4E′). The different FtsZ localization patterns in these two situations (before and after rescue) support our hypothesis that the rescue of the double mutant by MinC/MinD is due to the redistribution of FtsZ molecules in the cell that allow assembly of functional Z rings at internal sites.

## DISCUSSION

The current view on the action of the Min system suggests that Z rings formed at any position in the cell have equal sensitivity to MinC/MinD in the absence of the topological regulator MinE. However, in this study, we provided evidence that in *E. coli* polar divisions are more susceptible to MinC/MinD, even in the absence of MinE. First, a level of MinC/MinD could be found to completely block minicell formation in several Δ*min* strains without causing any filamentation, indicating that polar divisions are efficiently blocked under these situations although internal divisions are not affected. Immunostaining analyses confirmed that MinC/MinD works at the level of Z ring formation to differentially affect divisions at different positions. Second, a level of MinC/MinD induction was found to rescue the growth of the *min slmA* double mutant at low temperature. This was an unexpected result if we did not consider the different MinC/MinD sensitivities of polar and internal Z rings. The lethality of this double mutant appears to be the inability to assemble functional Z rings due to FtsZ being spread among multiple nonfunctional FtsZ structures in the absence of these Z ring regulators. Consistent with this explanation, additional FtsZ can rescue this double mutant (3). If additional FtsZ is needed to help these cells grow, how can MinC/MinD, a potent inhibitor of Z ring assembly, rescue the growth of these mutants? We suggest that rescue is due to a proper level of MinC/MinD selectively disrupting polar Z rings (or FtsZ polymer structures near cell poles before a polar Z ring is made), therefore making sufficient FtsZ available for internal Z ring assembly as though FtsZ molecules released from the polar Z rings/FtsZ structures are squeezed into internal spaces.

Among all of the strains tested, BSM374 displayed the greatest difference in MinC/MinD sensitivities between polar and internal Z rings. A broad range of MinC/MinD induction levels can stop minicell production in this strain without causing filamentation, and at relatively high levels, MinC/MinD can completely revert the morphology of this strain to a WT morphology. Thus, the function of MinE can be totally bypassed in achieving spatial regulation of Z ring assembly in this strain (Fig. 1). This raises the question of why such a complex oscillation arose through evolution when a single mutation in FtsZ can achieve the same result without Min oscillation. The chloroplast MinD from *Arabidopsis thaliana* ($_{At}$MinD) is able to interact with *E. coli* MinC and reduce minicell production in a *min* mutant in the absence of MinE, producing a near-wild-type morphology (42). In this case, $_{At}$MinD displays dramatic polar localization, whereas in our case, MinC/MinD was not concentrated at poles (see below).

Surprisingly, the minimal MinC/MinD level required to stop minicell production in the BSM374 strain was not much higher than for the FtsZ-WT strain S4 (with plasmid pBANG59, 50 μM IPTG was required to stop minicell formation in BSM374

and 20 μM was required for S4) (Fig. 1A and 3A), which means that polar Z rings in BSM374 do not have much more resistance to MinC/MinD than those in the S4 strain. Again, this was something unexpected, because the BSM374 strain displayed significant MinC/MinD resistance compared to the S4 strain in a killing assay performed previously (36). These seemingly contradictory observations actually support our finding that polar and internal Z rings have different sensitivities to MinC/MinD, although the extent of the differences can vary between strains. The killing assay actually measures the sensitivity of internal Z rings to MinC/MinD, since this determines the viability of the strain. The BSM374 strain survives high levels of MinC/MinD induction, indicating that internal Z rings in this strain have significant resistance to MinC/MinD. But, as evidenced by the ability of a low level of MinC/MinD to block minicell formation, the polar Z rings in this strain (BSM374) do not have much more MinC/MinD resistance than the polar Z rings in the S4 strain. These comparisons clearly demonstrate that the differences in MinC/MinD sensitivities between polar and internal Z rings are amplified in the BSM374 strain. However, it is not clear why the difference is much greater in the BSM374 strain than in other strains.

MinC-MTS, like MinC/MinD, is able to selectively block polar divisions, but MinC by itself does not. Within a limited range, MinC-MTS, but not MinC, is also able to rescue the double mutant S16 (*ftsZ-I374V min*::*kan slmA*::*cat*) (data not shown). These results imply that MinD is not absolutely required but that MinC has to be on the membrane to differentiate polar and internal Z rings. However, two pieces of information suggest that MinD is doing something else to aid MinC in distinguishing polar and internal Z rings. First, as mentioned above, although MinC-MTS is able to stop minicell formation in the BSM374 strain (Fig. 2), it can never convert this strain to a WT-like morphology as MinC/MinD does. Second, the rescue of S16 (*ftsZ-I374V min*::*kan slmA*::*cat*) by MinC-MTS is not as efficient as by MinC/MinD, because some of the cells are still filamentous even under the best rescue conditions. The failure of MinC by itself, or SulA, to preferentially disrupt polar Z rings and rescue the *min slmA* double mutant may be because MinC and SulA are in the cytoplasm, where they target cytoplasmic FtsZ forms (monomer and/or polymer forms) that are the precursors of Z rings. These precursors are unlikely to be presorted and differentially directed to specific locations in the cell but are probably shared by all potential Z rings. Therefore, when MinC or SulA is induced to decrease the supply of Z ring precursors, polar and internal Z rings are equally affected.

MinC has two functional domains, and both domains are required for the proper function of the Min system (16, 35, 44). However, in the context of our tests, $MinC^{N}$ seems to play a more important role than $MinC^{C}$ in disrupting polar Z rings. First, the plasmid pBANG59 containing the MinC-R172A mutation (which abolishes the FtsZ-$MinC^{C}$/MinD interaction) was able to reduce minicell production significantly in the S4 and BSM374 strains (data not shown); however, the same plasmid harboring the MinC-G10D mutation (which reduces the activity of $MinC^{N}$) only mildly decreased minicell formation in those two strains, even at the maximal induction level (Fig. 1 and 3). Second, in the double mutant rescue assay, MinC/MinD and $MinC^{R172A}$/MinD efficiently rescued the strain S14 (*ftsZ-WT min*::*kan slmA*::*cat*) as well as S16 (*ftsZ-I374V min*::*kan slmA*::*cat*), indicating that an active $MinC^{N}$ is sufficient. In contrast, $MinC^{G10D}$/MinD did not rescue these mutants (Fig. 4B), and MinC/MinD did not rescue the S19 strain (*ftsZ-N280D min*::*kan slmA*::*cat*) efficiently (the N280D mutation makes FtsZ resistant to $MinC^{N}$) (Fig. 4A). These data suggest that $MinC^{N}$ plays a critical role in the rescue of these double mutant strains, because when the action of $MinC^{N}$ is reduced (by mutations in MinC or FtsZ), the rescue is never very efficient.

It would be interesting to know the molecular basis for the different MinC/MinD sensitivities between polar and internal Z rings. There are at least two possibilities: either MinC/MinD works more efficiently at cell poles even in the absence of MinE, or the midcell/internal location is the preferred place for Z ring assembly and midcell/internal Z rings are better protected against the attack of MinC/MinD. In support of the first possibility, as mentioned above, the chloroplast MinD localizes to and recruits *E. coli* MinC to the *E. coli* cell poles efficiently, making polar but not midcell Z rings sensitive to $_{At}$MinD/$_{Ec}$MinC in the absence of MinE (42). *E. coli* MinD may have a similar preference (localizing to the pole) as $_{At}$MinD. In support of this, cardiolipin (CL) was shown to be enriched at *E. coli* cell poles (but also at septum [24, 29]), and MinD seems to have a higher affinity for CL than other phospholipids such as phosphatidylglycerol (PG). This implies that MinC/MinD would localize to and be concentrated at cell poles. However, fluorescence microscopy analysis of GFP-MinD and GFP-MinC/MinD (or GFP-$MinC^{C}$/MinD) in Δ*min* cells revealed that the GFP signal was not enriched at cell poles but was evenly distributed on the membrane (35, 43). Additionally, as discussed above, MinD does not seem to be absolutely required for MinC to selectively disrupt the polar Z rings, because MinC-MTS can do it efficiently in the absence of MinD. This MinC-MTS fusion seems to be evenly distributed on the membrane too, as revealed by GFP tagging at the N terminus. Deletion of the gene for cardiolipin synthesis, *cls* (which is responsible for the majority of CL synthesis [34]), in the S4 and BSM374 strains did not affect the localization pattern of GFP-MinD or the changes in morphology these strains undergo upon MinC/MinD induction (data not shown). Thus, there is no evidence that MinC/MinD is significantly enriched at cell poles, which might preferentially disrupt polar Z rings. However, this does not completely rule out the possibility that MinC/MinD works more efficiently at cell poles. There might be a polarly localized factor(s) that activates or increases the affinity of MinC/MinD for FtsZ without enriching MinC/MinD at the poles. However, genes for such factors have not yet been identified.

In Δ*min* strains, the Z rings are predicted to randomly form at polar and internal positions between nucleoids, because the frequency of polar divisions (about 30% of total divisions) in these cells is consistent with such a "random formation" model, based on calculations from the heterogeneous cell length distribution of these cells (for example, a cell with one length unit has one middle and two polar positions for potential Z ring formation, and a cell with two length units will have three middle/internal and two polar positions, etc). In such a model the midpoint of the cell is not preferred for Z ring assembly in the absence of the Min system (39). However, this

may or may not be the case; experimental data that fit a model do not mean that the model is correct. For instance, when the *min slmA* double mutant is grown at 42°C, not very many minicells (less than with regular Δ*min* strains) are produced, and the majority of the divisions (and Z rings too, as revealed by immunostaining) are between nucleoids at internal positions (data not shown). This seems to suggest that middle/internal spaces are preferred for Z ring assembly and subsequent division. As for the possibility that internal Z rings are better protected against MinC/MinD, we think it's possible, even though there is no evidence indicating that this is the case. If it is true, there must be factors (proteins, special biophysical properties of the middle area of the cell, etc.) involved that differentiate the midcell Z ring from polar Z rings. We examined ZapA, which is recruited to the Z ring by direct interaction with FtsZ, but we found that deletion of *zapA* did not affect the change in morphology of BSM374 upon MinC/MinD induction (data not shown).

In *B. subtilis*, the negative Z ring regulators EzrA and MinC/MinD also seem to have stronger effects on polar Z rings than on midcell Z rings, but the mechanism is not very clear either (10, 25). MinJ and DivIVA appear to block the action of MinC/MinD on constricting Z rings/septa under physiological conditions. MinC/MinD is localized to the Z ring/septum by MinJ-DivIVA as constriction initiates, but it never disrupts the Z ring (10). Instead, it prevents the disassembling Z ring from reforming adjacent to the completed septum (12). However, in the absence of MinJ or DivIVA, MinC/MinD is delocalized and disrupts Z rings and therefore causes filamentation (6, 30). So, during division, MinJ-DivIVA works to protect the constricting Z rings from being disrupted by MinC/MinD. There is a fundamental difference in the way MinC/MinD localization is controlled between *E. coli* and *B. subtilis*. *E. coli* has MinE, which restricts MinC/MinD to the poles through oscillation. It does not have the MinJ-DivIVA system. However, similar factors may exist to better protect the midcell Z rings against MinC/MinD in *E. coli*. In support of this, Juarez and Margolin (23) reported that the oscillating MinC/MinD may pause at midcell close to the septum during constriction. If so, a MinJ-DivIVA-like function would be needed to protect the constricting Z rings from being destroyed at midcell by the paused MinC/MinD. It will be interesting to determine the identities of these factors. Nevertheless, even if such factors exist, their protection is limited, because the differences in MinC/MinD sensitivity between polar and internal Z rings are not as great in the FtsZ-WT strain as in the FtsZ-I374V strain.

Returning to the original question, we ask: why do the two FtsZ mutants (BSZ280D and BSZ374) fail to produce minicells, whereas the two MinC mutants (MinC-G10D and MinC-R172A) do, even though they display significant resistance to MinC/MinD? Information collected from this study indicates that one contributing factor is that the Z rings formed at polar and internal positions have different sensitivities to MinC/MinD. For instance, in the FtsZ-I374V mutant, the polar Z rings are not much more resistant to MinC/MinD than polar Z rings in an FtsZ-WT strain, although the midcell ones are significantly more resistant. Therefore, in the BSZ374 strain, MinC/MinD concentrated at cell poles through the Min oscillation eliminates polar Z rings efficiently, and minicells are not produced. Because of the different MinC/MinD sensitivities between polar and internal Z rings, the requirements for MinC/MinD to disrupt Z rings formed at different cellular locations may also be different. This may partially explain why FtsZ mutants behave differently than MinC mutants in terms of minicell production.

## ACKNOWLEDGMENT

This work was supported by National Institutes of Health grant GM029764.

## REFERENCES

1. **Adams, D. W., and J. Errington.** 2009. Bacterial cell division: assembly, maintenance and disassembly of the Z ring. Nat. Rev. Microbiol. **7:**642–653.
2. **Bendezu, F. O., C. A. Hale, T. G. Bernhardt, and P. A. de Boer.** 2009. RodZ (YfgA) is required for proper assembly of the MreB actin cytoskeleton and cell shape in E. coli. EMBO J. **28:**193–204.
3. **Bernhardt, T. G., and P. A. de Boer.** 2005. SlmA, a nucleoid-associated, FtsZ binding protein required for blocking septal ring assembly over Chromosomes in E. coli. Mol. Cell **18:**555–564.
4. **Bi, E., and J. Lutkenhaus.** 1993. Cell division inhibitors SulA and MinCD prevent formation of the FtsZ ring. J. Bacteriol. **175:**1118–1125.
5. **Bi, E. F., and J. Lutkenhaus.** 1991. FtsZ ring structure associated with division in Escherichia coli. Nature **354:**161–164.
6. **Bramkamp, M., et al.** 2008. A novel component of the division-site selection system of Bacillus subtilis and a new mode of action for the division inhibitor MinCD. Mol. Microbiol. **70:**1556–1569.
7. **Dajkovic, A., and J. Lutkenhaus.** 2006. Z ring as executor of bacterial cell division. J. Mol. Microbiol. Biotechnol. **11:**140–151.
8. **Dajkovic, A., A. Mukherjee, and J. Lutkenhaus.** 2008. Investigation of regulation of FtsZ assembly by SulA and development of a model for FtsZ polymerization. J. Bacteriol. **190:**2513–2526.
9. **de Boer, P. A., R. E. Crossley, and L. I. Rothfield.** 1989. A division inhibitor and a topological specificity factor coded for by the minicell locus determine proper placement of the division septum in E. coli. Cell **56:**641–649.
10. **Edwards, D. H., and J. Errington.** 1997. The Bacillus subtilis DivIVA protein targets to the division septum and controls the site specificity of cell division. Mol. Microbiol. **24:**905–915.
11. **Fu, X., Y. L. Shih, Y. Zhang, and L. I. Rothfield.** 2001. The MinE ring required for proper placement of the division site is a mobile structure that changes its cellular location during the Escherichia coli division cycle. Proc. Natl. Acad. Sci. U. S. A. **98:**980–985.
12. **Gregory, J. A., E. C. Becker, and K. Pogliano.** 2008. Bacillus subtilis MinC destabilizes FtsZ-rings at new cell poles and contributes to the timing of cell division. Genes Dev. **22:**3475–3488.
13. **Hale, C. A., and P. A. de Boer.** 1997. Direct binding of FtsZ to ZipA, an essential component of the septal ring structure that mediates cell division in E. coli. Cell **88:**175–185.
14. **Hale, C. A., H. Meinhardt, and P. A. de Boer.** 2001. Dynamic localization cycle of the cell division regulator MinE in Escherichia coli. EMBO J. **20:**1563–1572.
15. **Hu, Z., E. P. Gogol, and J. Lutkenhaus.** 2002. Dynamic assembly of MinD on phospholipid vesicles regulated by ATP and MinE. Proc. Natl. Acad. Sci. U. S. A. **99:**6761–6766.
16. **Hu, Z., and J. Lutkenhaus.** 2000. Analysis of MinC reveals two independent domains involved in interaction with MinD and FtsZ. J. Bacteriol. **182:**3965–3971.
17. **Hu, Z., and J. Lutkenhaus.** 2001. Topological regulation of cell division in E. coli spatiotemporal oscillation of MinD requires stimulation of its ATPase by MinE and phospholipid. Mol. Cell **7:**1337–1343.
18. **Hu, Z., and J. Lutkenhaus.** 1999. Topological regulation of cell division in Escherichia coli involves rapid pole to pole oscillation of the division inhibitor MinC under the control of MinD and MinE. Mol. Microbiol. **34:**82–90.
19. **Hu, Z., A. Mukherjee, S. Pichoff, and J. Lutkenhaus.** 1999. The MinC component of the division site selection system in Escherichia coli interacts with FtsZ to prevent polymerization. Proc. Natl. Acad. Sci. U. S. A. **96:**14819–14824.
20. **Hu, Z., C. Saez, and J. Lutkenhaus.** 2003. Recruitment of MinC, an inhibitor of Z-ring formation, to the membrane in Escherichia coli: role of MinD and MinE. J. Bacteriol. **185:**196–203.
21. **Huisman, O., R. D'Ari, and S. Gottesman.** 1984. Cell-division control in Escherichia coli: specific induction of the SOS function SfiA protein is sufficient to block septation. Proc. Natl. Acad. Sci. U. S. A. **81:**4490–4494.
22. **Ivanov, V., and K. Mizuuchi.** 2010. Multiple modes of interconverting dynamic pattern formation by bacterial cell division proteins. Proc. Natl. Acad. Sci. U. S. A. **107:**8071–8078.
23. **Juarez, J. R., and W. Margolin.** 2010. Changes in the Min oscillation pattern before and after cell birth. J. Bacteriol. **192:**4134–4142.
24. **Koppelman, C. M., T. Den Blaauwen, M. C. Duursma, R. M. Heeren, and N.**

**Nanninga.** 2001. Escherichia coli minicell membranes are enriched in cardiolipin. J. Bacteriol. **183:**6144–6147.
25. **Levin, P. A., I. G. Kurtser, and A. D. Grossman.** 1999. Identification and characterization of a negative regulator of FtsZ ring formation in Bacillus subtilis. Proc. Natl. Acad. Sci. U. S. A. **96:**9642–9647.
26. **Loose, M., E. Fischer-Friedrich, J. Ries, K. Kruse, and P. Schwille.** 2008. Spatial regulators for bacterial cell division self-organize into surface waves in vitro. Science **320:**789–792.
27. **Lutkenhaus, J.** 2007. Assembly dynamics of the bacterial MinCDE system and spatial regulation of the Z ring. Annu. Rev. Biochem. **76:**539–562.
28. **Meinhardt, H., and P. A. de Boer.** 2001. Pattern formation in Escherichia coli: a model for the pole-to-pole oscillations of Min proteins and the localization of the division site. Proc. Natl. Acad. Sci. U. S. A. **98:**14202–14207.
29. **Mileykovskaya, E., and W. Dowhan.** 2000. Visualization of phospholipid domains in Escherichia coli by using the cardiolipin-specific fluorescent dye 10-N-nonyl acridine orange. J. Bacteriol. **182:**1172–1175.
30. **Patrick, J. E., and D. B. Kearns.** 2008. MinJ (YvjD) is a topological determinant of cell division in Bacillus subtilis. Mol. Microbiol. **70:**1166–1179.
31. **Pichoff, S., and J. Lutkenhaus.** 2002. Unique and overlapping roles for ZipA and FtsA in septal ring assembly in Escherichia coli. EMBO J. **21:**685–693.
32. **Raskin, D. M., and P. A. de Boer.** 1999. MinDE-dependent pole-to-pole oscillation of division inhibitor MinC in Escherichia coli. J. Bacteriol. **181:**6419–6424.
33. **Raskin, D. M., and P. A. de Boer.** 1999. Rapid pole-to-pole oscillation of a protein required for directing division to the middle of Escherichia coli. Proc. Natl. Acad. Sci. U. S. A. **96:**4971–4976.
34. **Romantsov, T., et al.** 2007. Cardiolipin promotes polar localization of osmosensory transporter ProP in Escherichia coli. Mol. Microbiol. **64:**1455–1465.
35. **Shen, B., and J. Lutkenhaus.** 2009. The conserved C-terminal tail of FtsZ is required for the septal localization and division inhibitory activity of MinC(C)/MinD. Mol. Microbiol. **72:**410–424.
36. **Shen, B., and J. Lutkenhaus.** 2010. Examination of the interaction between FtsZ and $MinC^N$ in E. coli suggests how MinC disrupts Z rings. Mol. Microbiol. **75:**1285–1298.
37. **Shiomi, D., and W. Margolin.** 2007. The C-terminal domain of MinC inhibits assembly of the Z ring in Escherichia coli. J. Bacteriol. **189:**236–243.
38. **Szeto, T. H., S. L. Rowland, C. L. Habrukowich, and G. F. King.** 2003. The MinD membrane targeting sequence is a transplantable lipid-binding helix. J. Biol. Chem. **278:**40050–40056.
39. **Teather, R. M., J. F. Collins, and W. D. Donachie.** 1974. Quantal behavior of a diffusible factor which initiates septum formation at potential division sites in Escherichia coli. J. Bacteriol. **118:**407–413.
40. **Weiss, D. S., J. C. Chen, J. M. Ghigo, D. Boyd, and J. Beckwith.** 1999. Localization of FtsI (PBP3) to the septal ring requires its membrane anchor, the Z ring, FtsA, FtsQ, and FtsL. J. Bacteriol. **181:**508–520.
41. **Wu, L. J., and J. Errington.** 2004. Coordination of cell division and chromosome segregation by a nucleoid occlusion protein in Bacillus subtilis. Cell **117:**915–925.
42. **Zhang, M., Y. Hu, J. Jia, H. Gao, and Y. He.** 2009. A plant MinD homologue rescues Escherichia coli HL1 mutant (ΔMinDE) in the absence of MinE. BMC Microbiol. **9:**101.
43. **Zhou, H., and J. Lutkenhaus.** 2003. Membrane binding by MinD involves insertion of hydrophobic residues within the C-terminal amphipathic helix into the bilayer. J. Bacteriol. **185:**4326–4335.
44. **Zhou, H., and J. Lutkenhaus.** 2005. MinC mutants deficient in MinD- and DicB-mediated cell division inhibition due to loss of interaction with MinD, DicB, or a septal component. J. Bacteriol. **187:**2846–2857.